

Relativistic magnetic reconnection in laser-microplasma interaction

Longqing Yi¹ and Tünde Fülöp¹

¹ *Department of Physics, Chalmers University of Technology, Göteborg, Sweden*

Relativistic magnetic reconnection (RMR) is a process that usually occurs in strongly magnetised astrophysical environments, when the magnetic energy per particle exceeds the rest mass energy, i.e. the magnetisation parameter $\sigma = B^2/4\pi nm_e c^2 \geq 1$, where B is the magnetic field strength, m_e is the electron mass, n is the plasma density, and c is the vacuum light velocity. Recently, it has been demonstrated experimentally that such conditions can be achieved by a high intensity laser interacting with a plasma [1]. Laboratory realization of RMR may help answering open questions, such as the reconnection rate and the associated particle acceleration.

For many astrophysical processes, σ is typically 100-1000 [2], and achieving such values in laboratory plasmas requires high laser energy. For single X-line reconnection considered in previous laser-plasma reconnection experiments, the minimum energy required for RMR is $\varepsilon_{\min} \sim \lambda_p^3 B^2 / 4\pi \propto \sigma n^{-1/2}$, where λ_p is the plasma wavelength. Thus a laser interacting with specially designed micro-scale structures, allowing for depositing laser energy in a small volume ($\sim \lambda_p^3$) of high-density plasma, is the most economic choice for such experiments.

In our recent work [3], we considered RMR triggered by laser driven electron beams on the surfaces of a micro-sized plasma slab [4]. Three-dimensional (3D) particle-in-cell (PIC) simulations show that when the electron beams approach the end of the plasma, due to the decreasing of plasma density, the electron number in the local plasma becomes insufficient to form a return current that is strong enough to separate the currents. The two electron beams attract each other due to Ampère's force law, and the magnetic field lines that move with the electrons are pushed together and reconnect. The RMR leads to the emission of relativistic electron jets with cut-off energy ~ 10 MeV, which propagate backwards (with respect to the laser propagation) and towards the exhaust of reconnection site.

The electron jets with ~ 10 MeV energy can easily penetrate the main target, and can be distinguished from all the other fast electrons by their energy range and angular distribution. They provide the basic means of diagnostics of RMR in laser-microplasma interaction. Therefore it should be of great interest to detect such electron jets in experiments. In this paper, we focus on the possibility of experimental implementation of the scheme proposed in Ref. [3], with some adjustments to adapt to current experimental capabilities.

Simulation of laser-wire interaction Figure 1 shows an example based on laser interaction with a micro-sized wire target. Instead of a slab that was used in the scheme presented

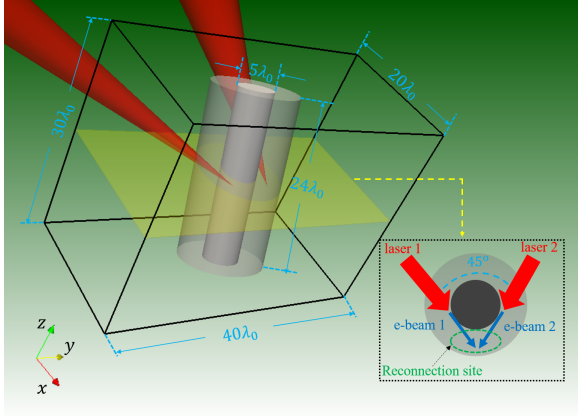


Figure 1: Schematic of the simulation setup. Two laser pulses (red-cones) irradiate a wire (white cylinder) on each side and drive two electron beams which trigger RMR when they interact at the back side of the wire. The semi-transparent structure around the wire is the density-decreasing ramp due to the heating of laser pre-pulse. The black frame is the simulation box, and the simulation parameters are marked in the figure. The inset is a 2D illustration of the process showing the cross-section marked by the yellow plane in the main figure.

in Ref. [3], the target is now a micro-scale plasma wire. Such target can be easily produced and has been used in previous experiments [5]. The wire target has a radius of $r_0 = 2.5\lambda_0$, and a length of $24\lambda_0$, where $\lambda_0 = 0.8\mu\text{m}$ is the laser wavelength. The density of the wire is $n_0 = 10n_c$ within the diameter ($r \leq r_0$), and decreases exponentially as $n = n_0 \exp[(r - r_0)^2/\sigma_0^2]$ as r increases, where $\sigma_0 = 2\lambda_0$ and $n_c = m_e \omega_0^2 / 4\pi e^2$ is the critical density. Such a density ramp could be produced by the laser pre-pulse. The wire is placed with 18° angle with respect to the laser-incident plane (x - y plane in Fig. 1) to avoid the reflected laser pulses destroying the optics.

The region when the two laser driven beams meet behind the wire is the reconnection site (as illustrated in the inset of Fig. 1). The two electron beams that trigger RMR are driven by two laser pulses irradiating the wire with an angle of 45° in between. The lasers are linearly polarised in the x - y plane, and the intensity, spot size and duration (FWHM) of each laser pulse are $I_0 = 4.3 \times 10^{19} \text{ W/cm}^2$, $w_0 = 2.8\mu\text{m}$, and $\tau_0 = 27 \text{ fs}$, respectively. Synchronisation of two lasers can be challenging, but it has been demonstrated in previous experiments [6].

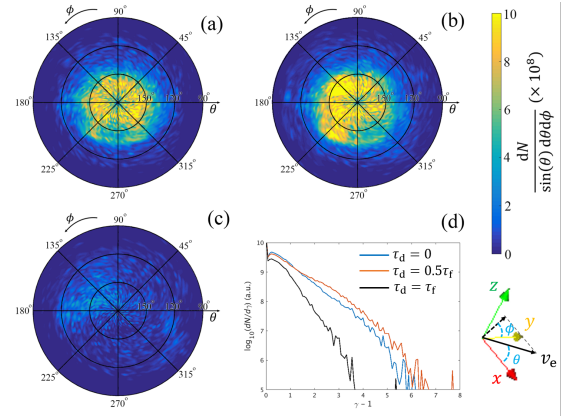


Figure 2: Reconnection signatures from the laser-wire setup. Angular distribution of the relativistic electrons (kinetic energy $E_k > m_e c^2$) received at the $-x$ boundary of the simulation box, for different temporal delays between the two laser pulses (a) $\tau_d = 0$, (b) $\tau_d = 0.5\tau_f$, and (c) $\tau_d = \tau_f$. The angles θ and ϕ are defined in the bottom-right, where v_e is the electron velocity, θ is the angle between v_e and $+x$ direction, and ϕ is the angle between the projection of v_e in the transverse plane (yz) with $+y$ direction. (d) The energy spectrum of the electrons in the three cases.

By adjusting the temporal delay of (τ_d) of two laser pulses, three simulations are performed for $\tau_d = 0$, $\tau_d = 0.5\tau_f$, and $\tau_d = \tau_f$, where $\tau_f \approx 3\tau_0$ is the full duration of the laser pulses. Note that the interaction between laser-driven beams, and therefore reconnection, can only happen when $\tau_d < \tau_f$, which allows us to perform some simple null tests. The simulations are performed by the EPOCH PIC code [7]. The size of the simulation box is $x \times y \times z = 20\lambda_0 \times 40\lambda_0 \times 30\lambda_0$, sampled by $400 \times 800 \times 600$ cells, with 5 macro electrons per cell. Immobile ions are used to improve computational efficiency.

Figure 2 shows the angular distribution of electron jets produced by the RMR as well as the energy spectrum. Figures 2 (a) and (b) show that there is a significant boost in the backward-propagating electrons yield when the two lasers overlap temporally, and Fig. 2(d) shows that these two cases have very similar energy spectrum with cut-off kinetic energy ~ 3 MeV. In contrast, Fig. 2(c) shows a dramatic decrease of the electron yield when the temporal delay of the two laser pulses is greater than the duration. In this case, the cut-off energy is only about half of that in the other two cases. This indicates that the observed feature is a signature of RMR triggered by the laser-driven electron beams in the middle.

Discussion Comparing with the simulations presented in the Supplementary Information of Ref. [3], the results shown here are based on a slightly different setup and diagnostics, and as expected the results are also somewhat different. The most important difference is that the angular distribution patterns of the electron jets [shown in Fig. 2(a) and (b)] are not evidently extended in $\pm z$ direction ($\phi = 90^\circ$ and 270°). This is counterintuitive because the magnetic tension force at the reconnection site tends to disperse the electrons towards the reconnection exhaust in those directions. However, this is just a result of different diagnostic method. In Ref. [3], the electron jets were shown when they were generated in the simulation box. But the "final" distribution pattern that will be detected depends also on the propagation afterwards, especially the scattering by the charge-separation fields near the wire. Here, we consider the electrons that escape from the simulation box, and record their energy and momentum when they are leaving the simulation box (assuming that they move straight afterwards). However, note, that in the near-critical-density (NCD) layer of the plasma density ramp (semi-transparent cylinder in Fig. 1), strong surface currents are excited, which are mostly guided by the wire and eventually escape from the simulation box from the upper ($+z$) and lower ($-z$) boundary as shown in Fig. 3. These surface electrons are abundant and mixed with the reconnection-associated jets that are emitted with $\theta \sim 90^\circ$ along $\pm z$ direction. Therefore in Fig. 2 we only take into account the electrons escaping from $-x$ boundary (dark surface in Fig. 3), and the extended part in the angular distribution pattern is not captured.

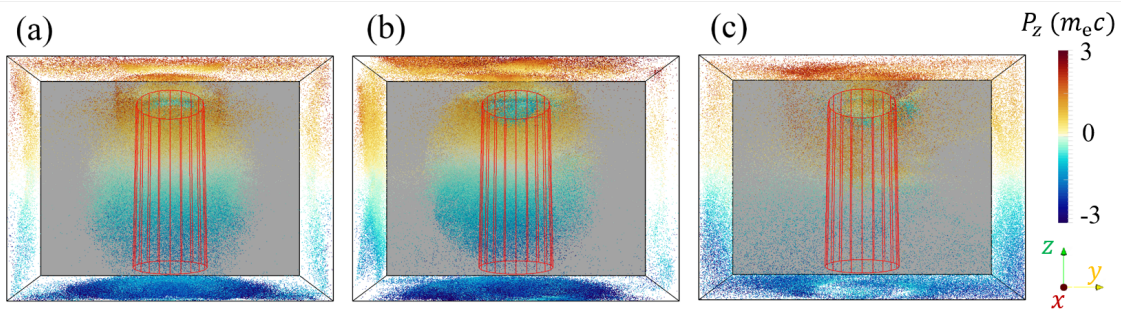


Figure 3: Electrons that escape from the simulation box (view from $+x$ direction), for the cases $\tau_d = 0$ (a), $\tau_d = 0.5\tau_f$ (b), and $\tau_d = \tau_f$ (c). The position of the dots shows where the electrons left the box and the colour represents their momentum P_z . The $-x$ boundary is marked with dark colour, electrons escaping from here are recorded and used to plot Fig. 2. The red cylindrical frame in the middle shows the position of the wire target.

To get the full picture, we plot all the electrons that escape from the simulation box in Fig. 3, where the electrons are shown in the position from where they are escaping, and the colour represents their momentum in z direction (P_z). In Fig. 3(a) and (b) the electrons are concentrated in the back of the wire target, and those in Fig. 3(b) are slightly leaning towards the $-y$ direction due to the fact that the interaction of the two laser-driven electron beams is off-axis. On the other hand, the escaped electrons shown in Fig. 3(c) are much fewer and almost uniformly distributed. These electrons are not associated with reconnection, instead they come from the laser-driven surface electrons, as some of these are energetic enough to escape from the charge separation fields as they rotate around the wire target.

In summary, the RMR does not depend crucially on the detailed structure of micro-sized plasma target, which indicates that the underlying physical process is robust. Experimental implementation of the scheme should be possible with two laser pulses interacting with a wire.

Supported by the Knut and Alice Wallenberg Foundation. Simulations performed on resources at Chalmers Centre for Computational Science and Engineering (C3SE) provided by the Swedish National Infrastructure for Computing (SNIC). Conference attendance is supported by Kungl. Vetenskaps- och Vitterhets-Samhället i Göteborg.

References

- [1] A. Raymond et al., arXiv:1610.06866, (2017).
- [2] H. Ji et al., Phys. Plasmas **18**, 6 (2011).
- [3] L. Q. Yi et al., Nat. Communications **9**, 1601 (2018).
- [4] L. Q. Yi et al., Phys. Rev. Letts. **116**, 115001 (2016).
- [5] M. Borghesi et al., Phys. Plasmas **9**, 2214 (2002).
- [6] B. Aurand et al., Phys. Plasmas **23**, 023113 (2016).
- [7] T. D. Arber, Plasma Phys. Control. Fusion. **57**, 113001 (2015).